

---

# Robust Normalizing Flows using Bernstein-type Polynomials

---

**Sameera Ramasinghe \***

The Australian National University, Data61-CSIRO  
sameera.ramasinghe@anu.edu.au

**Kasun Fernando \***

University of Toronto

**Salman Khan**

Mohamed Bin Zayed University of AI

**Nick Barnes**

The Australian National University

## Abstract

Modeling real-world distributions can often be challenging due to sample data that are subjected to perturbations, *e.g.*, instrumentation errors, or added random noise. Since flow models are typically nonlinear algorithms, they amplify these initial errors, leading to poor generalizations. This paper proposes a framework to construct Normalizing Flows (NF), which demonstrates higher robustness against such initial errors. To this end, we utilize Bernstein-type polynomials inspired by the optimal stability of the Bernstein basis. Further, compared to the existing NF frameworks, our method provides compelling advantages like theoretical upper bounds for the approximation error, higher interpretability, suitability for compactly supported densities, and the ability to employ higher degree polynomials without training instability. We conduct a thorough theoretical analysis and empirically demonstrate the efficacy of the proposed technique using experiments on both real-world and synthetic datasets.

## 1 Introduction

Modeling the probability distribution of a set of observations, *i.e.*, generative modeling, is a crucial task in machine learning. It enables the generation of synthetic samples using the learned model and allows the estimation of the likelihood of a data sample. This field has met with great success in many problem domains including image generation [Ho et al., 2019, Kingma and Dhariwal, 2018, Lu and Huang, 2020], audio synthesis [Esling et al., 2019, Prenger et al., 2019], reinforcement learning [Mazouze et al., 2020, Ward et al., 2019], noise modeling [Abdelhamed et al., 2019], and simulating physics experiments [Wirnsberger et al., 2020, Wong et al., 2020]. In the recent past, deep neural networks such as generative adversarial networks (GANs) and variational autoencoders (VAEs) have been widely adopted in generative modeling due to their success in modeling high dimensional distributions. However, they entail several limitations: 1) exact density estimation of arbitrary data points is not possible, and 2) training can be cumbersome due to aspects such as mode collapse, posterior collapse and high sensitivity to architectural design of the model [Kobyzev et al., 2020].

In contrast, normalizing flows (NFs) are a category of generative models that enable exact density computation and efficient sampling. As a result, NFs have been gaining increasing attention from the machine learning community since the seminal work of Rezende and Mohamed [2015]. In essence, NFs consist of a series of diffeomorphisms that transform a simple distribution into a more complex one, and must be designed so that the Jacobian determinants of these diffeomorphisms can

---

\*The authors contributed equally.

be efficiently calculated (This is, in fact, an essential part of the implementation). To this end, two popular approaches have been proposed so far: 1) efficient determinant calculation methods such as Berg et al. [2018], Grathwohl et al. [2018], Lu and Huang [2020], and 2) *triangular maps* [Jaini et al., 2019, Dinh et al., 2014, 2016]. The key benefit of triangular maps is that their Jacobian matrices are triangular, and hence, the calculation of Jacobian determinants takes only  $O(n)$  steps as opposed to the  $O(n^3)$  complexity of the computation of a determinant of an unconstrained  $n \times n$ -matrix. In this paper, we focus only on triangular maps.

However, it is not a priori clear whether such a constrained class of maps is expressive enough to produce sufficiently complex transformations. Interestingly, [Bogachev et al., 2005] shows that, given two probability densities, there exists a unique increasing triangular map that transforms one density to the other. Consequently, the constructed NFs should be *universal*, i.e., dense in the class of increasing triangular maps, in order to approximate those density transformations with arbitrary precision. But it is observed in Jaini et al. [2019] that, despite many NFs being triangular, they are not universal. To remedy this, most have reverted to the empirical approach of stacking several transformations together, thereby increasing the expressiveness of the model. Alternatively, there are NFs that use genuinely universal transformations. Many such methods employ coupling functions based on polynomials, e.g., sum-of-squares (SOS) polynomials in Jaini et al. [2019], cubic splines in Durkan et al. [2019a] or rational quadratic splines in Durkan et al. [2019b]. Here, we employ another class of polynomials called Bernstein-type polynomials to construct a universal triangular flow. Our universality proof, unlike in the previous literature, is constructive, and hence, yields analytic expressions for approximations of known density transformations; see Section 3.3.

It is also possible that just like any other nonlinear model, NFs are susceptible of numerical instabilities. In fact, it is well-known that nonlinear models could amplify initial errors and produce drastically different outcomes even for small changes in the input data; see Taylor [1982], Higham [1996], Lanckriet et al. [2002]. Therefore, the numerical instability of an NF model is an obstruction to the reproducibility of results as well as the generalization of the model to other sample sets or real-world data. Then, it is imperative that the robustness of NFs is investigated during their construction and implementation. Despite this obvious importance, robustness of NFs has not been theoretically or even experimentally studied in the previous literature. One of the key motivations behind this work was to fill this void. Accordingly, we show that Bernstein-type polynomials are ideal candidates for the construction of NFs that are not only universal but also robust. Robustness of Bernstein-type NFs follow from the *optimal stability* of the Bernstein basis [Farouki and Goodman, 1996, Farouki and Rajan, 1987]; see also, Section 3.4.

Apart from collecting, organizing and summarising in a coherent fashion the appropriate theoretical results which were scattered around the mathematical literature, we

- prove in Theorem 1 that in *any* NF it is enough to consider compactly supported targets (which in the previous literature was implicitly assumed without proper justification),
- extend, in Theorem 2, the monotonicity result of Bernstein polynomials in Lindvall [2002], to show the strict monotonicity, and hence, the invertibility of the model, and
- prove, in Theorem 3, the universality of Bernstein flows by extending a well-known theorem in Bernstein [1912].

Further, we believe that our work is the first to discuss a theoretical bound for the rate of convergence and error upper-bounds of NF models; see Section 3.3. In fact, we show that our method, in practice, performs better than this bound; see Section 5.3. Moreover, thanks to known mathematical properties of polynomials being used as building blocks, any polynomial based model, in particular, our MF model is highly interpretable (see Jaini et al. [2019] and Section 3.5). Compared to previous NF models, our method has several additional advantages such as suitability for approximating compactly supported target densities; see Section 3.1, the ability to increase the expressiveness by increasing the polynomial degree at no cost to the training stability; see Section 3.1, and being able to invert easily and accurately due to the availability of efficient root finding algorithms; see Section 3.2.

## 2 Preliminaries

In this section, we describe the general set up of triangular normalizing flow models and introduce Bernstein-type polynomials. The notation introduced in this section will be used throughout the paper.

## 2.1 Normalizing flows and triangular maps

NFs learn an invertible mapping between a prior and a more complex distribution (the target) in the same dimension. Typically, the prior is chosen to be a Gaussian with identity covariance or uniform on the unit cube, and the target is the one we intend to learn. Below, we present a summary of related ideas and refer the readers to [Jaini et al. \[2019\]](#) and [Kobyzev et al. \[2020\]](#) for a comprehensive discussion.

More formally, let  $\mathbf{z}$  and  $\mathbf{x}$  be sampled data from the prior with density  $P_z$  and the target distribution with density  $P_x$ , respectively. Then, NFs learn a transformation  $f$  such that  $f(\mathbf{z}) = \mathbf{x}$  which is differentiable and invertible with a differentiable inverse. Such transformations are called diffeomorphisms and they allow the estimation of the probability density  $P_x(\mathbf{x})$  via the change of variables formula  $P_x(\mathbf{x}) = P_z(f^{-1}\mathbf{x})|\mathbf{J}_f(f^{-1}\mathbf{x})|^{-1}$  where  $\mathbf{J}_f$  is the Jacobian determinant of  $f$ .

Given an independent and identically distributed (i.i.d.) sample  $\{x_1, \dots, x_n\}$  with law  $P_x$ , learning the target density  $P_x$  and the transformation  $f$  (within an expressive function class  $\mathfrak{F}$ ) is done simultaneously via minimizing the Kullback-Leibler (KL) divergence between  $P_x$  and the pushforward of  $P_z$  under  $f$  denoted by  $f_*P_z$ ,

$$\min_{f \in \mathfrak{F}} \text{KL}(P_x \| f_*P_z) = - \max_{f \in \mathfrak{F}} \int \log \frac{P_z(f^{-1}\mathbf{x})}{|\mathbf{J}_f(f^{-1}\mathbf{x})|} \cdot P_x(\mathbf{x}) d\mathbf{x}. \quad (1)$$

Density estimation using (1) requires efficient calculation of the Jacobian as well as  $f^{-1}$ . Both can be achieved via constraining  $f$  to be an *increasing triangular map*. That is, taking  $P_x(\mathbf{x})$  to be a multivariate distribution where  $\mathbf{x} = (x_1, x_2, \dots, x_d)$ , and the prior  $P_z(\mathbf{z})$  where  $\mathbf{z} = (z_1, z_2, \dots, z_d)$ , the components of  $\mathbf{x}$  are expressed as  $x_j = f_j(z_1, z_2, \dots, z_j)$  for suitably defined transformations  $f_j, j = 1, 2, \dots, d$  where  $f_j$  is increasing with respect to  $z_j$ . From now on, we denote  $(z_1, z_2, \dots, z_j)$  by  $z_{<j+1}$ . In this case, the Jacobian determinant is the product  $\prod_{j=1}^d \partial_{z_j} f_j$ . Also, because  $f_j$  is increasing in  $z_j$ , inversion can be done recursively starting from  $f_1^{-1}$ .

## 2.2 Bernstein-type polynomials

Bernstein polynomials (of degree  $n$ ),  $\binom{n}{k}x^k(1-x)^{n-k}$ ,  $0 \leq k \leq n$ ,  $n \in \mathbb{N}$ , were first introduced by Bernstein in his constructive proof of the Weierstrass theorem in [Bernstein \[1912\]](#). In fact, given a continuous function  $f : [0, 1] \rightarrow \mathbb{R}$ , its degree  $n$  Bernstein approximation,  $B_n(f) : [0, 1] \rightarrow \mathbb{R}$ , given by

$$B_n(f)(x) = \sum_{k=0}^n f\left(\frac{k}{n}\right) \binom{n}{k} x^k (1-x)^{n-k}, \quad (2)$$

is such that  $B_n(f) \rightarrow f$  uniformly in  $[0, 1]$  as  $n \rightarrow \infty$ . Moreover, Bernstein polynomials form a basis for degree  $n$  polynomials on  $[0, 1]$ . More generally, polynomials of Bernstein-type can be defined as follows.

**Definition 1.** A degree  $n$  polynomial of Bernstein-type is a polynomial of the form

$$B_n(x) = \sum_{k=0}^n \alpha_k \binom{n}{k} x^k (1-x)^{n-k}, \quad x \in [0, 1] \quad (3)$$

where  $\alpha_k, 0 \leq k \leq n$  are some real constants.

**Remark 1.** Polynomials of Bernstein-type on an arbitrary closed interval  $[a, b]$  are defined by composing  $B_n$  with the linear map that sends  $[a, b]$  to  $[0, 1]$ ,  $L_{a,b}(x) = \frac{x-a}{b-a}$ . So, Bernstein-type polynomials on  $[a, b]$  take the form

$$B_n \circ L_{a,b}(x) = \sum_{k=0}^n \alpha_k \binom{n}{k} \frac{(x-a)^k (b-x)^{n-k}}{(b-a)^n}. \quad (4)$$

Hereafter, we denote degree  $n$  Bernstein-type polynomials by  $B_n$  regardless of the domain.

As we shall see below, one can control various properties of Bernstein-type polynomials like strict monotonicity, range and universality by specifying conditions on the coefficients, and the error of approximation depends on the degree of the polynomials used.

### 3 Theoretical Foundations of the Bernstein-type Normalizing Flow

Here, we elaborate on the desirable properties of Bernstein-type polynomials and their implication to our NF model. The mathematical results taken directly from existing literature are stated with appropriate references. The proofs of novel results, Theorems 1, 2 and 3, appear in Appendix A. Also, in each subsection, we point out the advantages of our model (over existing models) based on the properties discussed.

#### 3.1 Range and compact targets

The supports of distributions of samples used when training and applying NFs are not fixed. So, it is important to be able to easily control the range of the coupling functions. In the case of Bernstein-type polynomials,  $B_n$ s, this is very straight-forward. Note that if  $B_n$  is defined on  $[a, b]$ , then  $B_n(a) = \alpha_0$  and  $B_n(b) = \alpha_n$ . Therefore, one can fix the values of a Bernstein-type polynomial at the end points of  $[a, b]$  by fixing  $\alpha_0$  and  $\alpha_n$ . So, if  $B_n$  is increasing (which will be the case in our model; see Section 3.2), then its range is  $[\alpha_0, \alpha_n]$ . This translates to a significant advantage when training for compactly supported targets because we can achieve any desired range  $[c, d]$  (the support of the target) by fixing  $\alpha_0 = c$  and  $\alpha_n = d$  and letting only  $\alpha_k$ ,  $0 < k < n$  vary. So,  $B_n$ s are ideal for modeling compactly supported targets. In fact, in most other methods except splines in Durkan et al. [2019a,b], either there is no obvious way to control the range or the range is infinite.

We present the following theorem to establish that for the purpose of training, we can assume the target has compact support (up to a known diffeomorphism).

**Theorem 1.** *Let  $I_j$ ,  $j = 1, 2, 3$  be measurable subsets of  $\mathbb{R}^d$ . Suppose  $I_1$  is the support of the target  $P_x$ ,  $I_2$  is the support of the prior  $P_z$ ,  $\mathfrak{F}$  is the class of coupling functions with ranges contained in  $I_3$  and  $h : I_3 \rightarrow I_1$  is a diffeomorphism. If  $P_y$  is the distribution on  $I_3$  such that  $h_*P_y = P_x$ , then*

$$\arg \min_{f \in \mathfrak{F}} \text{KL}(P_x \| (h \circ f)_* P_z) = \arg \min_{f \in \mathfrak{F}} \text{KL}(P_y \| f_* P_z)$$

Therefore, our coupling functions having finite ranges is not a restriction, and in *any* NF model, even if the target density is not compactly supported, the learning procedure can be implemented by first converting the target density to a density with a suitable compact support via a diffeomorphism, and then training on the transformed data.

Since we deal with compactly supported targets, in practice, we do not need to construct deep architectures (with a higher number of layers), as we can increase the degree of the polynomials to get a better approximation. In other polynomial based methods, a practical problem arises because the higher order polynomials could predict extremely high values initially leading to unstable gradients. In contrast, we can avoid that problem as the range of our transformations can be explicitly controlled from the beginning by fixing  $\alpha_0$  and  $\alpha_n$ .

#### 3.2 Strict monotonicity and inversion

In triangular flows, the coupling maps are expected to be invertible. Since, strict monotonicity implies invertibility it is sufficient that the  $B_n$ s we use are strictly monotone. Below, by extending a result in Lindvall [2002], we specify a (surprisingly simple) condition that guarantees this.

**Theorem 2.** *Consider the Bernstein-type polynomial  $B_n$  in (3). Suppose  $\alpha_0 < \alpha_1 < \dots < \alpha_n$ . Then  $B_n$  is strictly increasing on  $[0, 1]$ .*

According to this result, the strict monotonicity of  $B_n$ s depends entirely on the strict monotonicity of the coefficients  $\alpha_k$ s. Further, it follows that the assumption of strict monotonicity of the coefficients is not a further restriction on the optimization problem (1). For example, if the required range is  $[c, d]$ , we can take  $\alpha_{n-k} = c + (d - c)(1 + v_0^2 + \dots + v_k^2)^{-1}$  where  $v_k$ s are real valued. This converts the constrained problem of finding  $\alpha_k$ s to an unconstrained one of finding  $v_k$ s. Alternatively, we can take  $\alpha_0 = c$  and  $\alpha_k = |v_1| + \dots + |v_k|$ , and after each iteration, linearly scale  $\alpha_k$ s in such a way that  $\alpha_n = d$ .

After guaranteeing invertibility, we focus on computing the inverse, i.e., at each iteration, given  $x$  we solve for  $z \in [0, 1]$ ,  $B_n(z) = \sum_{k=0}^n \alpha_k \binom{n}{k} z^k (1 - z)^{n-k} = x$ . This is equivalent to solving  $\sum_{k=0}^n (\alpha_k - x) \binom{n}{k} z^k (1 - z)^{n-k} = 0$  because Bernstein polynomials form a partition of unity on  $[0, 1]$ . So, finding inverse images, i.e., solving the former is equivalent to finding solutions to the

latter. Due to our assumption of increasing  $\alpha_k$ s,  $B_n$  is increasing, and has at most one root on  $[0, 1]$ . The condition  $(\alpha_0 - x)(\alpha_n - x) < 0$  (which can be easily checked) guarantees the existence of a unique solution, and hence, the invertibility of the original transformation.

Due to the extensive use of Bernstein-type polynomials in computer-aided geometric design, there are several well-established efficient root finding algorithms at our disposal [Spencer, 1994]. For example, the parabolic hull approximation method in Rajan et al. [1988] is ideal for higher degree polynomials with fewer roots (in our case, just one) and has cubic convergence for simple roots (better than both the bijection method and Newtons method). Further, because of the numerical stability described in Section 3.4 below, the use of Bernstein-type polynomials in our model minimizes the errors in such root solvers based on floating-point arithmetic.

Even though inverting splines are easier due to the availability of analytic expressions for roots, compared to all other other NF models, we have more efficient and more numerically stable algorithms that allow us to reduce the cost of numerical inversion in our setting.

### 3.3 Universality and the convergence rate

In order to guarantee universality of triangular flows, we need to use a class of coupling functions that well-approximates increasing continuous functions. This is, in fact, the case for  $B_n$ s. To see this, recall from Bernstein [1912] that  $B_n$ s are uniformly dense in the space of continuous function on  $[0, 1]$ . By rescaling, this is true on any interval  $[a, b]$ . Moreover, by construction, whenever  $f$  is increasing,  $B_n(f)$  is increasing. So, it is automatic that increasing Bernstein polynomials on  $[a, b]$  are uniformly dense in the space of increasing continuous functions, and in particular, in the space increasing differentiable maps on  $[a, b]$  (as required). The equation (4) gives us the explicit formula for the  $B_n$  that approximates  $f$ . Finally, to show true universality, we have to show that any increasing continuous function  $f : \mathbb{R} \rightarrow \mathbb{R}$  is well-approximated by  $B_n$ s. This is our next result.

**Theorem 3.** *Let  $f : \mathbb{R} \rightarrow \mathbb{R}$  be continuous. Then there is a sequence of Bernstein-type polynomials that converges to  $f$  point-wise on  $\mathbb{R}$  and converges uniformly to  $f$  on any compact set.*

The basis of all the previous proofs of universality and ours is the fact that the learnable class of functions is dense in the class of increasing continuous functions. However, the argument we present is constructive. So, as shown below in Section 3.6, we can write down sequences of approximations for (known) transformations between densities.

In the case of cubic splines of Durkan et al. [2019a], it is known that for  $k = 1, 2, 3$  and 4, when the transformation is  $k$  times continuously differentiable and the bin size is  $h$ , the error is  $O(h^k)$  [Ahlberg et al., 1967, Chapter 2]. However, we are not aware of any other instance where an error bound is available. Fortunately for us, the error of approximation of a function  $f$  by its Bernstein polynomials has been extensively studied. We state one such result due to Voronovskaya [1932] and refer to Bustamante [2017, Chapter 4] for its proof and a detailed account of other error bounds.

**Theorem 4** (Voronovskaya). *Suppose  $f : [0, 1] \rightarrow \mathbb{R}$  is twice continuously differentiable. Then*

$$B_n(f) - f = \frac{x(1-x)}{2n} f''(x) + o(n^{-1}).$$

*and this error cannot be improved by increasing the smoothness of  $f$ .*

**Remark 2.** *This holds for an arbitrary interval  $[a, b]$  with  $x(1-x)$  replaced by  $(x-a)(b-x)$ .*

Since the error estimate is given in terms of the degree of the polynomials used, we can improve the optimality of our NF by avoiding unnecessarily high degree polynomials. This allows us to keep the number of trainable parameters under control in our NF model.

The following example shows that the error  $O(n^{-1})$  in Theorem 4 does not necessarily improve when SOS polynomials are used instead.

**Example 1.** Uniform $[0, 1]$  to the Normal $(0, 1)$  : *There is a bounded positive sequence  $\{c_k\}_{k \geq 0}$  s.t.*

$$f(z) = \text{Erf}^{-1}(2z - 1) = \sum_{k=0}^{\infty} \frac{\sqrt{2}\pi^{k+\frac{1}{2}}c_k}{2k+1} \left(z - \frac{1}{2}\right)^{2k+1};$$

*see Jaini et al. [2019]. This is the power series expansion of  $f$  at  $z = 1/2$ , and hence, it is unique. The SOS approximation of  $f$  (the series above truncated at  $k = n$ ) is only  $O((2n+1)^{-1}) = O(n^{-1})$  accurate on any compact sub-interval of  $(0, 1)$ . This is precisely the accuracy one would expect from the degree  $2n+1$  Bernstein approximation on any compact subinterval of  $(0, 1)$ .*



In our NF at each step the estimation is done using a univariate polynomial, and hence, the overall convergence rate is, in fact, the minimal univariate convergence rate of  $O(n^{-1})$ , (equivalently, the error upper bound is the maximum of univariate upper bounds) and in general, cannot be improved further regardless of how regular the density transformation is. However, our experiments (in Section 5.3) show that our model on average has a significantly smaller error than the given theoretical upper-bound.

### 3.4 Robustness

In this section, we recall some known results in Farouki and Goodman [1996], Farouki and Rajan [1987] about the optimal stability of the Bernstein basis. The two key ideas are that smaller *condition numbers* lead to smaller numerical errors and that the Bernstein basis has the optimal condition numbers compared to other polynomial bases.

To illustrate this, let  $p(x)$  be a polynomial on  $[a, b]$  of degree  $n$  expressed in terms of a basis  $\{\phi_k\}_{k=0}^n$ , i.e.,  $p(x) = \sum_{k=0}^n c_k \phi_k(x)$ ,  $x \in [a, b]$ . Let  $c_k$  be randomly perturbed, with perturbations  $\delta_k$  where the relative error  $\delta_k/c_k \in (-\epsilon, \epsilon)$ . Then the total pointwise perturbation is  $\delta(x) = \sum_{k=0}^n \delta_k \phi_k(x)$ . So,  $|\delta(x)| \leq \sum_{k=0}^n |\delta_k \phi_k(x)| \leq \epsilon \sum_{k=0}^n |c_k \phi_k(x)| \leq \epsilon C_\phi(p(x))$ , where  $C_\phi(p(x)) = \sum_{k=0}^n |c_k \phi_k(x)|$  is the condition number for the total perturbation with respect to the basis  $\phi_k$ . It is clear that  $C_\phi(p(x))$  controls the magnitude of the total perturbation.

The following result in Farouki and Goodman [1996] compares condition numbers with respect to two non-negative bases.

**Theorem 5** (Farouki & Goodman). *Suppose  $\phi = \{\phi_k\}_{k=0}^n$  and  $\psi = \{\psi_k\}_{k=0}^n$  are non-negative bases for polynomials of degree  $n$  on  $[a, b]$ . Suppose that for each  $j$ ,  $\psi_j$  is a non-negative linear combination of the former, that is,  $\psi_j = \sum_{k=0}^n M_{jk} \phi_k$  with  $M_{jk} \geq 0$ . Then for any polynomial  $p(x)$ ,  $C_\phi(p(x)) \leq C_\psi(p(x))$ .*

Let  $0 \leq a < b$ . On  $[a, b]$  the Bernstein polynomials and the power monomials,  $\{1, x, x^2, \dots, x^n\}$ , are non-negative bases. It is true that the latter is a positive linear combination of the former but not vice-versa; see Farouki and Goodman [1996]. So, we have the following Corollary.

**Corollary 1** (Farouki & Goodman). *Let  $0 \leq a < b$ ,  $\{\psi_k\}_{k=0}^n$  and  $\{\phi_k\}_{k=0}^n$  be the power basis and degree  $n$  Bernstein basis on  $[a, b]$  respectively. Then for any polynomial  $p(x)$ ,  $C_\phi(p(x)) \leq C_\psi(p(x))$ .*

This means that the change in the value of a polynomial caused by a perturbation of coefficients is always smaller in the Bernstein basis than in the power basis.

A more involved computation gives  $\tilde{C}_\phi(x_0) = (\frac{m!}{|p^{(m)}(x_0)|} \sum_{k=0}^n |c_k \phi_k(x_0)|)^{1/m}$  as the condition number that controls the computational error for a  $m$ -fold root  $x_0$  of  $p(x)$  in  $[a, b]$ ; see Farouki and Rajan [1987]. The following theorem establishes the robustness of the Bernstein basis for root finding.

**Theorem 6** (Farouki & Rajan). *For an arbitrary polynomial  $p(x)$  with a root  $x_0 \in [0, 1]$ , let  $\tilde{C}_\psi(x_0)$  and  $\tilde{C}_\phi(x_0)$  denote the condition numbers of the root in the power and the Bernstein bases on  $[0, 1]$ , respectively. Then  $\tilde{C}_\phi(x_0) < \tilde{C}_\psi(x_0)$  for  $x_0 \in (0, 1]$  and  $\tilde{C}_\phi(0) = \tilde{C}_\psi(0)$ .*

**Remark 3.** *In fact, the condition numbers of Bernstein basis on  $[a, b]$  are better than the condition numbers for the power basis adapted to  $[a, b]$ , i.e.,  $(x - a)^k$ ,  $k = 0, 1, \dots, n$  [Farouki and Rajan, 1987]. So, the above theorem does not depend on the choice of the interval  $[0, 1]$ .*

This means that the change in the value of a root of a polynomial caused by a perturbation of coefficients is always smaller in the Bernstein basis than in the power basis.

From the discussion, we conclude that Bernstein polynomial basis on a given interval is optimally stable, in the sense that no other non-negative basis gives smaller condition numbers for the values or roots of arbitrary polynomials on that interval. In particular,  $B_n$ s are systematically more stable than the polynomials in the power form when determining roots (for example, when inverting) and evaluation (for example, when finding image points). As a result, when polynomials are used to construct NFs, i.e., quadratic or cubic splines, SOS polynomials, and etc., Bernstein-type polynomials yield the most numerically stable NF. Our experiments in Section 5.2, while confirming this, demonstrates that our method outperforms even the NFs that are not based on polynomials.

### 3.5 Interpretability

Interpretability of NFs is determined by how much we know about the dependency of the properties of target distribution on the learnable parameters (in our case, coefficients of the polynomials). In general, polynomial based NFs are more interpretable than NAFs because we have knowledge of such dependencies, *e.g.*, coefficients of polynomials control the first few moments of the target density; see Jaini et al. [2019]. In our case, we can say more.

- If  $\alpha_k$ s are increasing, then so is  $B_n$ , and the support of the target density is  $[\alpha_0, \alpha_n]$ .
  - The condition numbers in Section 3.4 control the error of evaluation and inversion.
  - The approximation error corresponds to the degree of Bernstein-type polynomials in a precise way.
- Therefore, our model is highly interpretable.

### 3.6 Examples of Bernstein-type approximations

In this section, we illustrate how to use Bernstein-type polynomials to approximate diffeomorphisms between densities. We restrict our attention to densities on  $\mathbb{R}$ . Suppose  $F$  and  $G$  are the distribution functions of the two probability densities  $P_z$  and  $P_x$  on  $\mathbb{R}$ . Then the *increasing rearrangement*  $f = G^{-1} \circ F$  is the unique increasing transformation that pushes forward  $P_z$  to  $P_x$ , and this generalizes to higher dimensions [Villani, 2009, Chapter 1]. Now, using (4), we can explicitly write down their degree- $n$  Bernstein-type approximations,  $B_n(f)$  along with convergence rates.

**Example 2.** Uniform $[0, 1]$  to a continuous and non-zero density  $P$  on  $[0, 1]$  : Note that  $G(x) = \int_0^x P(s) ds$ ,  $x \in [0, 1]$  is strictly increasing and hence, invertible on  $[0, 1]$ . So,  $f(x) = G^{-1}(x)$ , and  $G^{-1}$  is once continuously differentiable. Then

$$B_n(f)(x) = \sum_{k=0}^n G^{-1}\left(\frac{k}{n}\right) \binom{n}{k} x^k (1-x)^{n-k}.$$

and  $\|B_n(f) - f\|_\infty = O(n^{-1/2})$ .

**Example 3.** Kumaraswamy $(\alpha, \beta)$  to Uniform $[0, 1]$  : Here,  $\alpha, \beta > 0$  and for  $x \in [0, 1]$ ,  $F(x) = 1 - (1 - x^\alpha)^\beta$  [Kumaraswamy, 1980] and  $G(x) = x$ . Therefore,  $f(x) = F(x)$ . Then

$$B_n(f)(x) = \sum_{k=0}^n F\left(\frac{k}{n}\right) \binom{n}{k} x^k (1-x)^{n-k}.$$

When  $\alpha, \beta \geq 1$ ,  $\|B_n(f) - f\| = O(n^{-1})$ .

## 4 Construction of the Bernstein-type Normalizing Flow

In this Section, we construct normalizing flows using the theoretical framework established in Section 3 for compactly supported targets. For this, we employ a MADE style network [Germain et al., 2015]. Consider a  $d$ -dimensional source  $P_z(\mathbf{z})$  and a  $d$ -dimensional target  $P_x(\mathbf{x})$ . Then, the element-wise mapping between the components  $x_j$  and  $z_j$  is approximated using a Bernstein-type polynomial as  $x_j = B_n^j(z_j)$ . We obtain the parameters of  $B_n^j(z_j)$  using a neural network which is conditioned on  $z_{<j}$ . This ensures a triangular mapping between the distributions.

We fix  $\alpha_0$  and  $\alpha_n$  to be constants, and thus, define the range of each transformation; see Section 3.1. Moreover, as per Theorem 2,  $\alpha_k$ s need to be strictly increasing for a transformation to be strictly increasing. However, when we convert this constrained problem to an unconstrained one as proposed in Section 3.2, we obtain  $v_k$ s using the neural network and then calculate  $\alpha_k$ s as described.

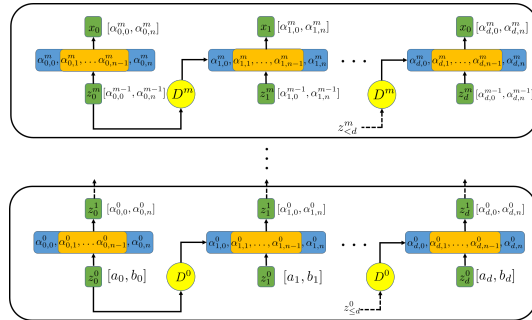


Figure 1: Overall Bernstein NF architecture with  $m+1$  layers for  $d$ -dimensional distributions. The ranges of transformations are within brackets and trainable coefficients are in orange boxes.

However, when we convert this constrained problem to an unconstrained one as proposed in Section 3.2, we obtain  $v_k$ s using the neural network and then calculate  $\alpha_k$ s as described.

For each  $B_n^j$ , we employ a fully-connected neural net with three layers to obtain the parameters, except in the case of  $B_n^0$  for which we directly optimize the parameters. Figure 1 illustrates a model architecture with  $m + 1$  layers and degree  $n$  polynomials for  $d$ -dimensional distributions. Here, there are  $(n - 1)(m + 1)$  variable coefficients altogether.

We use maximum likelihood to train the model with a learning rate 0.01 with a decay factor of 10% per 50 iterations. All the weights are initialized randomly using a standard normal distribution.

## 5 Experiments

In this section, we summarise our empirical evaluations of the proposed model based on both real-world and synthetic datasets and compare our results with other NF methods.

### 5.1 Modeling sample distributions

We conducted experiments on four datasets from the UCI machine-learning repository and BSDS300 dataset. Table 1 compares the obtained test log-likelihood against recent flow-based models. As illustrated, our model achieves competitive results on all of the five datasets. We observe that our model consistently reported a lower standard deviation which may be attributed to the robustness of our model.

We also applied our method to two low-dimensional image datasets, CIFAR10 and MNIST. The results are reported in Table 2. Among the methods that do not use multi-scale convolutional architectures, we obtain the optimal results. In addition, we tested our model on several toy datasets (shown in Figure 2). Note that these 2D datasets contain multiple modes, sharp jumps and are not fully supported. So, the densities are not that obvious to learn. Despite the difficulties, our model is able to estimate the given distributions in a satisfactory manner.

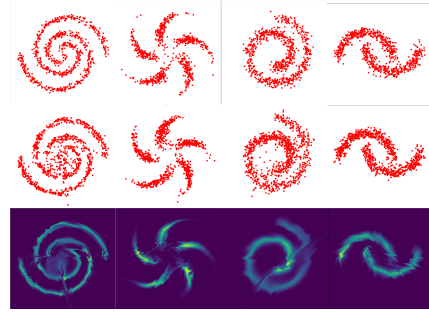


Figure 2: Qualitative results for modeling the toy distributions. *From the top row:* ground truth, prediction, and predicted density.

Table 1: Test log-likelihood comparison against the state-of-the-art on real-world datasets (higher is better). Results for competing methods are extracted from Durkan et al. [2019b] where error bars correspond to two standard deviations. Log-likelihoods are averaged over 10 trials for Bernstein.

MODEL	POWER	GAS	HEPMASS	MINIBOONE	BSDS300
FFJORD	$0.46 \pm 0.01$	$8.59 \pm 0.12$	$-14.92 \pm 0.08$	$-19.43 \pm 0.04$	$157.40 \pm 0.19$
GLOW	$0.42 \pm 0.01$	$12.24 \pm 0.03$	$-16.99 \pm 0.02$	$-10.55 \pm 0.45$	$156.95 \pm 0.28$
MAF	$0.45 \pm 0.01$	$12.35 \pm 0.02$	$-17.03 \pm 0.02$	$-10.92 \pm 0.46$	$156.95 \pm 0.28$
NAF	$0.62 \pm 0.01$	$11.96 \pm 0.33$	$-15.09 \pm 0.04$	$-8.86 \pm 0.15$	$157.73 \pm 0.04$
BLOCK-NAF	$0.61 \pm 0.01$	$12.06 \pm 0.09$	$-14.71 \pm 0.38$	$-8.95 \pm 0.07$	$157.36 \pm 0.03$
RQ-NSF (AR)	$0.66 \pm 0.01$	$13.09 \pm 0.02$	$-14.01 \pm 0.03$	$-9.22 \pm 0.48$	$157.31 \pm 0.28$
Q-NSF (AR)	$0.66 \pm 0.01$	$13.09 \pm 0.02$	$-14.01 \pm 0.03$	$-9.22 \pm 0.48$	$157.31 \pm 0.28$
SOS	$0.60 \pm 0.01$	$11.99 \pm 0.41$	$-15.15 \pm 0.10$	$-8.90 \pm 0.11$	$157.48 \pm 0.41$
BERNSTEIN	$0.63 \pm 0.01$	$12.81 \pm 0.01$	$-15.11 \pm 0.02$	$-8.93 \pm 0.08$	$157.13 \pm 0.11$

### 5.2 Robustness

In order to experimentally verify that Bernstein-type NFs are more numerically stable than other polynomial based NFs (as claimed in Section 3.4) we use a standard idea in the literature; see Taylor [1982]. We add i.i.d. noise (sampled from a Uniform[0, 0.01]) to the five datasets included in Table 1, and measure the change in the test log-likelihood as a fraction of the standard deviation (so that the change is in terms of standard deviations).

Table 2: Test log-likelihood comparison against the state-of-the-art on image datasets (higher is better). Results for competing methods are extracted from Jaini et al. [2019]. Note that the first three models use multi-scale convolutional architectures.

MODEL	MNIST	CIFAR10
REAL-NVP	-1.06	-3.49
FFJORD	-0.99	-3.40
GLOW	-1.05	-3.35
MAF	-1.89	-4.31
MADE	-2.04	-5.67
SOS	-1.81	-4.18
BERNSTEIN	-1.54	-4.04



For a fair comparison, we train all the models from the scratch over 5 trials to obtain the standard deviations and the test log-likelihoods. We used the codes provided by the authors, strictly following the instructions in the original works, to the best of our ability. Table 3 illustrates these results. As expected, Bernstein NF demonstrate the lowest relative change in performance, implying the robustness against random initial errors.

Table 3: Test log-likelihood drop for random initial errors, relative to the original standard deviations.

MODEL	POWER	GAS	HEPMASS	MINIBOONE	BSDS300
REAL-NVP	2.4	4.2	3.6	1.4	7.4
GLOW	2.1	4.1	2.3	0.8	6.9
MAF	2.4	4.4	3.9	0.8	7.1
MADE	2.1	4.6	3.6	2.4	8.1
RQ-NSF	2.3	5.4	4.1	0.9	7.8
SOS	2.1	1.7	1.9	1.6	6.1
BERNSTEIN	1.1	1.3	1.1	0.6	2.3

### 5.3 Validation of the theoretical error upper-bound

The degree  $n (\geq 5)$  Bernstein approximation of  $f \in C^3[0, 1]$  has an error upper-bound

$$E_n = n^{-1} \|\rho^2 f^{(2)}\|_\infty + n^{-3/2} \|\rho^3 f^{(3)}\|_\infty$$

where  $\rho(x) = \sqrt{x(1-x)}$  [Bustamante, 2017, Chapter 4]. This is an improved version of the Theorem 4. Now, we verify this experimentally using a KumarSwamy(2, 5) distribution as the prior and Uniform[0, 1] as the target; see Example 3.

Let  $f(x) = 1 - (1 - x^2)^5$  and  $B_n$  be the learned degree  $n$  Bernstein-type polynomial.

The average error,  $\int_0^1 |f(x) - B_n(x)| dx$ , obtained using the learned  $B_n$ s and  $E_n$  satisfying

$$1.25n^{-1} + 5n^{-3/2} < E_n < 1.25n^{-1} + 5.5n^{-3/2}$$

are plotted in Figure 3. It shows that the observed (average) error is smaller than this theoretical upper-bound.

In the NF, we have used a single layer and increased the degree of the polynomial from 10 to 100. The NF model was stable even when the degree 100 polynomial was used. So, this experiment also demonstrates that our model is, in fact, stable even when higher degree polynomials are used (as claimed in Section 3.1).

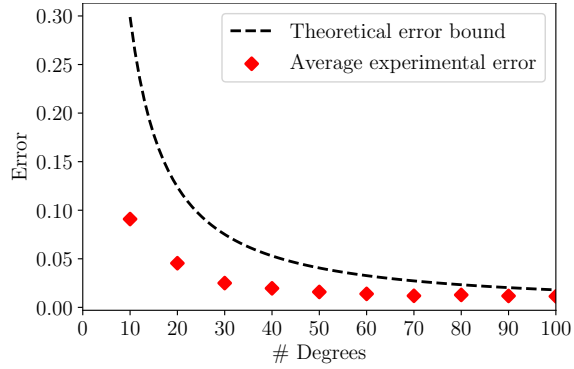


Figure 3: Error bound vs average experimental error.

## 6 Conclusion

In this paper, we proposed a novel method to construct a universal autoregressive normalizing flow with Bernstein-type polynomials as the coupling functions. Our theoretical discussion on Bernstein-type polynomials concluded that they possess properties ideal for constructing normalizing flows, and as a result, our method has several advantages like robustness against initial and round-off errors, higher interpretability, theoretical error bound, and better training stability for higher degree polynomials. We compared our method to other universal normalizing flows both theoretically and experimentally. Our experiments on real-world and synthetic datasets (including 2D multimodal ones) provided competitive results and show that our theoretical claims hold in practice.

## References

- Abdelrahman Abdelhamed, Marcus A Brubaker, and Michael S Brown. Noise flow: Noise modeling with conditional normalizing flows. In *Proceedings of the IEEE/CVF International Conference on Computer Vision*, pages 3165–3173, 2019.
- J. H. Ahlberg, E. N. Nilson, and J. L. Walsh. *The Theory of Splines and their Applications*. Academic Press, 1967.
- Rianne van den Berg, Leonard Hasenclever, Jakub M Tomczak, and Max Welling. Sylvester normalizing flows for variational inference. *arXiv preprint arXiv:1803.05649*, 2018.
- S. Bernstein. Démonstration du théorème de weierstrass fondée sur le calcul des probabilités. *Communications of the Kharkov Mathematical Society*, pages 1–2, 1912.
- Vladimir Igorevich Bogachev, Aleksandr Viktorovich Kolesnikov, and Kirill Vladimirovich Medvedev. Triangular transformations of measures. *Sbornik: Mathematics*, 196(3):309, 2005.
- J. Bustamante. *Bernstein Operators and Their Properties*. Birkhauser, 2017.
- Laurent Dinh, David Krueger, and Yoshua Bengio. Nice: Non-linear independent components estimation. *arXiv preprint arXiv:1410.8516*, 2014.
- Laurent Dinh, Jascha Sohl-Dickstein, and Samy Bengio. Density estimation using real nvp. *arXiv preprint arXiv:1605.08803*, 2016.
- Conor Durkan, Artur Bekasov, Iain Murray, and George Papamakarios. Cubic-spline flows. *arXiv preprint arXiv:1906.02145*, 2019a.
- Conor Durkan, Artur Bekasov, Iain Murray, and George Papamakarios. Neural spline flows. *arXiv preprint arXiv:1906.04032*, 2019b.
- Philippe Esling, Naotake Masuda, Adrien Bardet, Romeo Despres, et al. Universal audio synthesizer control with normalizing flows. *arXiv preprint arXiv:1907.00971*, 2019.
- R. T. Farouki and T. N. T. Goodman. On the optimal stability of the Bernstein basis. *Mathematics of Computation*, 65(216):1553—1566, 1996.
- R. T. Farouki and V. T. Rajan. On the numerical condition of polynomials in Bernstein form. *Computer Aided Geometric Design* 4, 4(3):191—216, 1987.
- Mathieu Germain, Karol Gregor, Iain Murray, and Hugo Larochelle. Made: Masked autoencoder for distribution estimation. In *International Conference on Machine Learning*, pages 881–889. PMLR, 2015.
- Will Grathwohl, Ricky TQ Chen, Jesse Bettencourt, Ilya Sutskever, and David Duvenaud. Ffjord: Free-form continuous dynamics for scalable reversible generative models. *arXiv preprint arXiv:1810.01367*, 2018.
- N. J. Higham. *Accuracy and stability of numerical algorithms*. SIAM, 1996.
- Jonathan Ho, Xi Chen, Aravind Srinivas, Yan Duan, and Pieter Abbeel. Flow++: Improving flow-based generative models with variational dequantization and architecture design. In *International Conference on Machine Learning*, pages 2722–2730. PMLR, 2019.
- Priyank Jaini, Kira A Selby, and Yaoliang Yu. Sum-of-squares polynomial flow. *arXiv preprint arXiv:1905.02325*, 2019.
- Diederik P Kingma and Prafulla Dhariwal. Glow: Generative flow with invertible 1x1 convolutions. *arXiv preprint arXiv:1807.03039*, 2018.
- Ivan Kobyzev, Simon Prince, and Marcus Brubaker. Normalizing flows: An introduction and review of current methods. *IEEE Transactions on Pattern Analysis and Machine Intelligence*, pages 1—1, 2020.
- P. Kumaraswamy. A generalized probability density function for double-bounded random processes. *Journal of Hydrology*, 46(1–2):79–88, 1980.
- G. R. G. Lanckriet, L. El Ghaoui, C. Bhattacharyya, and M. I. Jordan. A robust minimax approach to classification. *Journal of Machine Learning Research*, 3:555–582, 2002.
- T. Lindvall. *Lectures on the coupling method*. Dover Publications, 2002.

- You Lu and Bert Huang. Woodbury transformations for deep generative flows. *Advances in Neural Information Processing Systems*, 33, 2020.
- Bogdan Mazouze, Thang Doan, Audrey Durand, Joelle Pineau, and R Devon Hjelm. Leveraging exploration in off-policy algorithms via normalizing flows. In *Conference on Robot Learning*, pages 430–444. PMLR, 2020.
- Ryan Prenger, Rafael Valle, and Bryan Catanzaro. Waveglow: A flow-based generative network for speech synthesis. In *ICASSP 2019-2019 IEEE International Conference on Acoustics, Speech and Signal Processing (ICASSP)*, pages 3617–3621. IEEE, 2019.
- V. T. Rajan, S. R. Klinkner, and R. T. Farouki. Root isolation and root approximation for polynomials in Bernstein form. Technical Report RC14224, IBM Research Division, T. J. Watson Research Center, Yorktown Heights, N.Y. 10598, 1988.
- Danilo Jimenez Rezende and Shakir Mohamed. Variational inference with normalizing flows. *arXiv preprint arXiv:1505.05770*, 2015.
- M. R. Spencer. *Polynomial Real Root Finding in Bernstein Form*. PhD thesis, Brigham Young University, 1994.
- J. R. Taylor. *An introduction to error analysis: the study of uncertainties in physical measurements*. Mill Valley, Calif, University Science Books, 1982.
- Cédric Villani. *Optimal Transport: Old and New*. Springer, 2009.
- E. Voronovskaya. Détermination de la forme asymptotique d’approximation des fonctions par les polynômes de M. Bernstein. *Doklady Akademii Nauk SSSR*, pages 79—85, 1932.
- Patrick Nadeem Ward, Ariella Smofsky, and Avishek Joey Bose. Improving exploration in soft-actor-critic with normalizing flows policies. *arXiv preprint arXiv:1906.02771*, 2019.
- Peter Wirnsberger, Andrew J Ballard, George Papamakarios, Stuart Abercrombie, Sébastien Racanière, Alexander Pritzel, Danilo Jimenez Rezende, and Charles Blundell. Targeted free energy estimation via learned mappings. *The Journal of Chemical Physics*, 153(14):144112, 2020.
- Kaze WK Wong, Gabriella Contardo, and Shirley Ho. Gravitational-wave population inference with deep flow-based generative network. *Physical Review D*, 101(12):123005, 2020.

## Appendix

### 7 Proofs

*Proof of Theorem 1.* To illustrate the relevance of the theorem to our setting, we write down the details of the proof assuming that the learnable class  $\mathfrak{F}$  is Bernstein-type polynomials. The same proof is true for any class of functions.

Take  $I_j = [a_j, b_j]$  for  $j = 1, 2, 3$  with  $a_j < b_j$  with the possibility that  $a_1 = -\infty$  or  $b_1 = \infty$  whence the interval is understood to be open on the infinite end and the target may have non-compact support. Let  $B_n : I_2 \rightarrow I_3$  be the learnable Bernstein-type polynomial with coefficients  $\{\alpha_j\}_{j=0}^n$ . Let  $h : I_3 \rightarrow I_1$  be a fixed invertible transformation so that  $h^{-1}$  transforms the target density  $P_x$  to  $P_y$  supported on  $I_3$ , i.e.,  $h_* P_y = P_x$ , and

$$P_x(\mathbf{x}) = \frac{P_y(h^{-1}\mathbf{x})}{|\mathbf{J}_h(h^{-1}\mathbf{x})|}.$$

Fix  $\alpha_0 = a_3$ ,  $\alpha_n = b_3$  and let  $I = \{(\alpha_1, \dots, \alpha_{n-1}) \mid a_3 < \alpha_1 < \dots < \alpha_{n-1} < b_3\}$ . Then the optimization problem is

$$\begin{aligned} & \min_I \text{KL}(P_x \parallel (h \circ B_n)_* P_z) \\ &= -\max_I \int \log \frac{P_z(B_n^{-1}(h^{-1}\mathbf{x}))}{|\mathbf{J}_{h \circ B_n}(B_n^{-1}(h^{-1}\mathbf{x}))|} \cdot P_x(\mathbf{x}) d\mathbf{x} \\ &= -\max_I \int \log \frac{P_z(B_n^{-1}(h^{-1}\mathbf{x}))}{|\mathbf{J}_h(h^{-1}\mathbf{x})\mathbf{J}_{B_n}(B_n^{-1}(h^{-1}\mathbf{x}))|} \cdot P_x(\mathbf{x}) d\mathbf{x} \\ &= -\max_I \left\{ \int \log \frac{P_z(B_n^{-1}(h^{-1}\mathbf{x}))}{|\mathbf{J}_{B_n}(B_n^{-1}(h^{-1}\mathbf{x}))|} \cdot P_x(\mathbf{x}) d\mathbf{x} + \int \log |\mathbf{J}_h(h^{-1}\mathbf{x})| \cdot P_x(\mathbf{x}) d\mathbf{x} \right\} \quad (5) \\ &= -\max_I \left\{ \int \log \frac{P_z(B_n^{-1}(h^{-1}\mathbf{x}))}{|\mathbf{J}_{B_n}(B_n^{-1}(h^{-1}\mathbf{x}))|} \cdot \frac{P_y(h^{-1}\mathbf{x})}{|\mathbf{J}_h(h^{-1}\mathbf{x})|} d\mathbf{x} \right\} + \int \log |\mathbf{J}_h(h^{-1}\mathbf{x})| \cdot \frac{P_y(h^{-1}\mathbf{x})}{|\mathbf{J}_h(h^{-1}\mathbf{x})|} d\mathbf{x}. \\ &= -\max_I \left\{ \int \log \frac{P_z(B_n^{-1}(\mathbf{y}))}{|\mathbf{J}_{B_n}(B_n^{-1}(\mathbf{y}))|} \cdot P_y(\mathbf{y}) d\mathbf{y} \right\} + \int \log |\mathbf{J}_h(\mathbf{y})| \cdot P_y(\mathbf{y}) d\mathbf{x}. \\ &= \min_I \text{KL}(P_y \parallel (B_n)_* P_z) + \int \log |\mathbf{J}_h(\mathbf{y})| \cdot P_y(\mathbf{y}) d\mathbf{x} \quad (6) \end{aligned}$$

Note that the second integral in (5) can be taken outside the max because it is independent of  $B_n$ , and hence, it becomes a constant that is irrelevant for the optimization. From (6), it follows that the minimum of  $\text{KL}(P_x \parallel (h \circ B_n)_* P_z)$  is achieved if and only if the minimum of  $\text{KL}(P_y \parallel (B_n)_* P_z)$  is achieved. Hence,

$$\arg \min_I \text{KL}(P_x \parallel (h \circ B_n)_* P_z) = \arg \min_I \text{KL}(P_y \parallel (B_n)_* P_z) \quad (7)$$

as required. It is easy to see that this argument remains unchanged when  $B_n$  is replaced by  $f$  and  $I$  is replaced by  $f \in \mathfrak{F}$ .  $\square$

*Proof of Theorem 2.* There is a probabilistic interpretation of Bernstein polynomials that makes the analysis easier. Let  $Z_i^x$ ,  $0 \leq i \leq n$  be i.i.d. Bernoulli( $x$ ) random variables. Then

$$B_n(x) = \mathbb{E} \left( f \left( \sum_{i=0}^n Z_i^x / n \right) \right). \quad (8)$$

See, for example, Chapter 2 of [Bustamante \[2017\]](#). We will use this definition in the proof.

Let  $f : [0, 1] \rightarrow \mathbb{R}$  be a strictly increasing continuous function such that  $f(k/n) = \alpha_k$ . Let  $s < t$  and let  $Z_i^x$ ,  $0 \leq i \leq n$  and be a sequence of iid Bernoulli( $x$ ) for  $x = s, t$ , defined on the same probability space such that  $Z_i^s \leq Z_i^t$  via monotone coupling. That is, let  $Z_i^s = \mathbf{1}_{U \leq s}$  and  $Z_i^t = \mathbf{1}_{U \leq t}$  where  $U$  is a uniform random variables on  $[0, 1]$  and couple them as follows.

$$\mathbb{P}((Z_i^s, Z_i^t) = (j, k))_{j,k \in \{0,1\}} = \begin{pmatrix} 1-t & t-s \\ 0 & s \end{pmatrix}$$

and  $\mathbb{P}(Z_i^s > Z_i^t) = \mathbb{P}(Z_i^s = 1, Z_i^t = 0) = 0$ . So,  $Z_i^t \geq Z_i^s$  as required.

Then

$$f\left(\sum_{i=0}^n Z_i^s/n\right) \leq f\left(\sum_{i=0}^n Z_i^t/n\right).$$

Consequently,

$$\mathbb{E}\left(f\left(\sum_{i=0}^n Z_i^s/n\right)\right) \leq \mathbb{E}\left(f\left(\sum_{i=0}^n Z_i^t/n\right)\right). \quad (9)$$

Due to (8), this is equivalent to  $B_n(s) \leq B_n(t)$ .

If (9) is not strict, then  $f(\sum_{i=0}^n Z_i^t/n) = f(\sum_{i=0}^n Z_i^s/n)$  almost surely, and therefore,  $\sum_{i=0}^n Z_i^t = \sum_{i=0}^n Z_i^s$  almost surely. But this is impossible due to monotone coupling. Therefore, by contradiction, (9) is strict as required.  $\square$

*Proof of Theorem 3.* Choose two positive sequences  $\{M_n\}$  and  $\{\epsilon_n\}$  such that  $M_n \rightarrow \infty$  and  $\epsilon_n \rightarrow 0$ . Let  $I_n = [-M_n, M_n]$ . Then, there exists a Bernstein approximation  $q_n$  on  $I_n$  (which extends naturally to  $\mathbb{R}$ ) such that

$$\max_{I_n} |f - q_n| \leq \epsilon_n. \quad (10)$$

Then the sequence of Bernstein approximations  $\{q_n\}$  converges point-wise to  $f$  on  $\mathbb{R}$ , and this convergence is uniform on each compact interval.  $\square$

**Remark 4.** We can write down a sequence  $q_n$  explicitly when  $f$  is regular. For example, when  $f$  is  $C^3$  with bounded derivatives and  $M_n = \log n$ , choosing the degree of  $q_n$  to be  $n$  is sufficient because it follows from the error estimate in Section 5.3 that  $\epsilon_n \sim (\log n)/n$  works. That is, choose  $q_n$  to be the degree  $n$  Bernstein approximation of  $f$  on  $[-M_n, M_n]$ . Also, note that when  $f$  is increasing then  $q_n$  is increasing on  $[-M_n, M_n]$ .

## 1 Hyper-parameters and training details

For optimization, we used the Adam optimizer with parameters  $\beta_1 = 0.9$ ,  $\beta_2 = 0.999$ ,  $\epsilon = 1 \times 10^{-8}$ , where parameters refer to the usual notation. An initial learning rate of 0.01 was used for updating the weights with a decay factor of 10% per 50 iterations. We initialized all the trainable weights randomly from a standard normal distribution and used maximum likelihood as the objective function for training. We observed that a single layer model with 100 degree polynomials performed well for the real-world data. In contrast, for 2D toy distributions and images we used higher number of layers (8) with 15 degree polynomials in each layer. For all the experiments, we use a Kumaraswamy distribution with parameters  $a = 2$  and  $b = 5$  as the base density. Using a standard normal distribution after converting it to a density on  $[0, 1]$  using a nonlinear transformation, e.g.,  $\frac{1+\tanh(z)}{2}$ , also yielded similar results.

## 2 Training stability for higher degree polynomials

Typically, polynomial-based models such as SOS yield training instability as their target ranges are not compact. This is because higher degree approximations could increase the range of outputs without bound, and in turn cause gradients to explode while training. As a solution, they opt to use a higher number of layers with lower degree polynomials. In contrast, our model can entertain higher degree approximations without any instability which allows more design choices. Figure 4 demonstrates this behavior experimentally.

According to Figure 4, the model hits a peak in performance at a certain degree and shows a slight drop in performance at higher degrees. Nevertheless, the model does not exhibit unstable behavior at higher degrees as opposed to SOS-flows – an indication of the superior training stability of our model. This further illustrates that our model provides the option to design shallow models by increasing the number of degrees in the polynomials instead of deeper models with a higher number of layers.



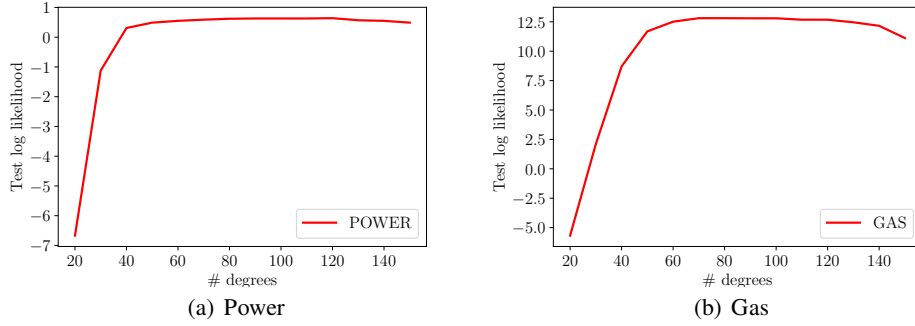


Figure 4: Test log-likelihood against the number of degrees used for the Bernstein approximation in a single layer model on POWER and GAS datasets. Slight dip in the performance for degrees 100+ but shows no training instability.

### 3 Ablation study

We compare the performance of different variants of our model against a simple task in order to better understand the design choices. For this, we use a standard normal as the base distribution, and a mixture of five Gaussians with means =  $(-5, -2, 0, 2, 5)$ , variances =  $(1.5, 2, 1, 2, 1)$ , and weights 0.2 each, as the target. Figure 5 depicts the results.

Clearly, we were able to increase the expressiveness of the transformation by increasing the degree of the polynomials, as well as the number of layers. However, it is also visible that using an unnecessarily higher degree over-parametrizes the model, and hence, deteriorate the output. As discussed in the main article and in Section 2, we are able to use polynomials with degree as high as 100 in this experiment and others with no cost to the training stability because the training is done for a compactly supported target.

We also examine how the initial base distribution affects the performance. We use a mixture of seven Gaussians with means =  $(-7, -5, -2, 0, 2, 5, 7)$ , variances =  $(1, 1, 2, 2, 2, 1, 1)$ , and weights =  $(0.8, 0.2, 0.2, 0.6, 0.2, 0.2, 0.8)$ , as the target. We used a model with a 100-degree polynomial and a single layer for this experiment. Figure 6 illustrates the results. Although all priors capture the multimodes, when Uniform $[0, 1]$  is used the model was not able to predict that the density is almost zero for large negative values.

### 4 Experiments with two-dimensional image datasets

In Table 2, we reported the results of the experiments we ran on two low-dimensional image datasets: CIFAR10 and MNIST. The samples generated from the experiment are shown Figure 7. We recall that we manage to obtain the optimal results among the methods that do not use multi-scale convolutional architectures.

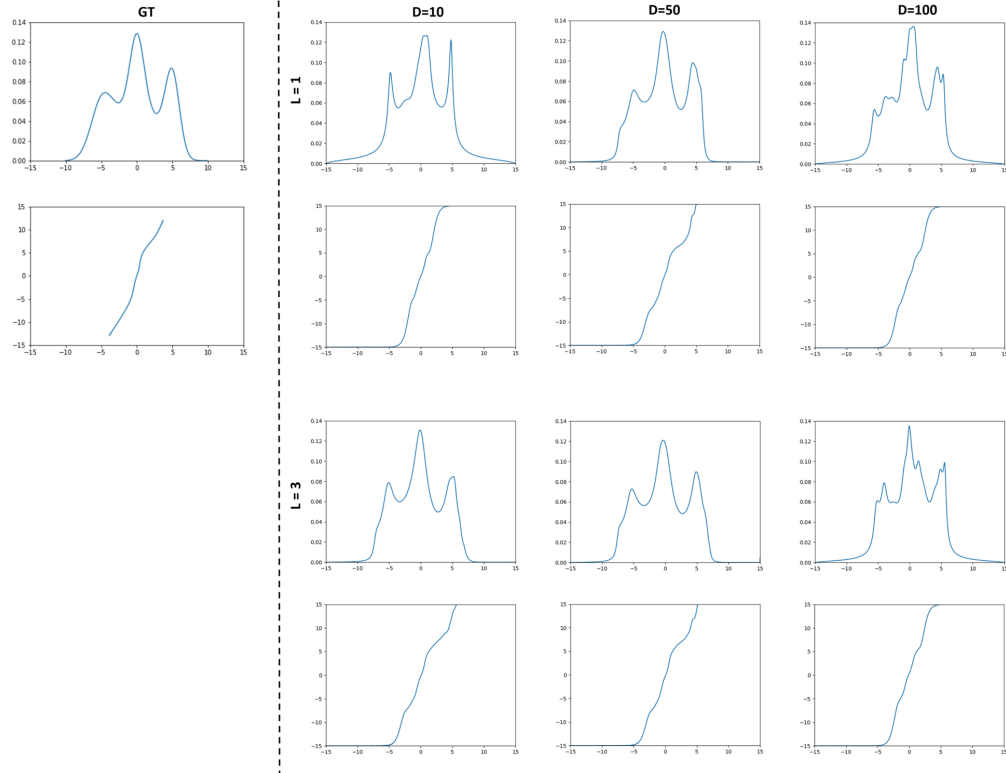


Figure 5: Ablation study with different variants of our model. **D** and **L** denotes the degree of the used polynomials and the number of layers, respectively. Corresponding transformation functions are also shown below the predicted densities.

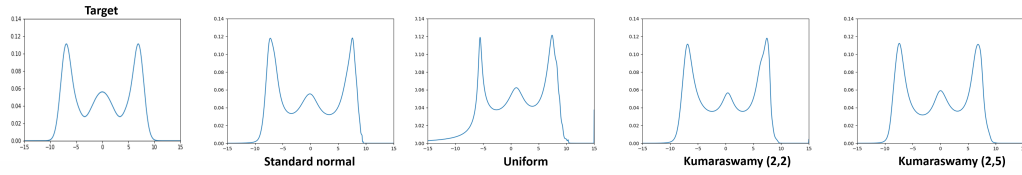


Figure 6: Approximation of the target density starting from various initial densities (the initial distributions are noted below the densities).



(a) MNIST

(b) CIFAR10

Figure 7: Generated samples on MNIST and CIFAR10.